

# The binary fraction of the young cluster NGC 1818 in the Large Magellanic Cloud

Y. Hu,<sup>1,2</sup> L. Deng,<sup>1</sup> Richard de Grijs,<sup>3,4,1</sup> Q. Liu,<sup>1,2</sup> and Simon P. Goodwin<sup>4</sup>

licai@bao.ac.cn

Received \_\_\_\_\_; accepted \_\_\_\_\_

---

<sup>1</sup>Key Laboratory of Optical Astronomy, National Astronomical Observatories, Chinese Academy of Sciences, Beijing 100012, P. R. China

<sup>2</sup>Graduate University of the Chinese Academy of Sciences, Beijing 100012, P. R. China

<sup>3</sup>Kavli Institute for Astronomy and Astrophysics, Peking University, Beijing 100871, P. R. China

<sup>4</sup>Department of Physics & Astronomy, The University of Sheffield, Sheffield S3 7RH, UK

## ABSTRACT

We use high-resolution *Hubble Space Telescope* imaging observations of the young ( $\sim 15 - 25$  Myr-old) star cluster NGC 1818 in the Large Magellanic Cloud to derive an estimate for the binary fraction of F stars ( $1.3 < M_*/M_\odot < 1.6$ ). This study provides the strongest constraints yet on the binary fraction in a young star cluster in a low-metallicity environment ( $[\text{Fe}/\text{H}] \sim -0.4$  dex). Employing artificial-star tests, we develop a simple method that can efficiently measure the probabilities of stellar blends and superpositions from the observed stellar catalog. We create synthetic color-magnitude diagrams matching the fundamental parameters of NGC 1818, with different binary fractions and mass-ratio distributions. We find that this method is sensitive to binaries with mass ratios,  $q \gtrsim 0.4$ . For binaries with F-star primaries and mass ratios  $q > 0.4$ , the binary fraction is  $\sim 0.35$ . This suggests a total binary fraction for F stars of 0.55 to unity, depending on assumptions about the form of the mass-ratio distribution at low  $q$ .

*Subject headings:* methods: statistical – binaries: general – galaxies: Magellanic Clouds – galaxies: star clusters: individual: NGC1818

## 1. Introduction

The majority of stars are thought to form in binary or multiple<sup>1</sup> systems (Goodwin & Kroupa 2005; Duchêne et al. 2007; Goodwin et al. 2007), and the initial binary properties of stars place important constraints on star formation and the origin of the stellar initial mass function (IMF; Goodwin et al. 2007, 2008). The majority of stars with masses greater than approximately  $0.5M_{\odot}$  are also thought to form in star clusters (Lada & Lada 2003), and the binary content of a star cluster plays an important role in both its observational properties and its dynamical evolution (e.g., Kroupa et al. 1999). In addition, many exotic objects observed in star clusters, such as blue stragglers, cataclysmic variables, and X-ray sources, are believed to be related to binary systems. Almost all studies of binarity have been limited to nearby, solar-metallicity populations. However, it might be expected that metallicity (e.g., through its effects on cooling and, hence, on the opacity limit for fragmentation) will play a role in the fragmentation of cores to produce binary systems (Bate 2005; Goodwin et al. 2007).

In general, the most direct way in which to study binary fractions is by examining whether a given star is part of a binary system, on an individual basis. Over the past two decades, the binary fractions of field stars in the solar neighborhood have been studied carefully in this conventional fashion (e.g., Abt 1983 for B stars; Duquennoy & Mayor 1991 for G dwarfs; Fischer & Marcy 1992 for M dwarfs; Kouwenhoven et al. 2006 for A and B stars; see also Goodwin et al. 2007 for a review). Nearby clusters and associations have also been examined in detail (see Duchêne 1999 and Duchêne et al. 2007 for reviews and comparisons). However, the binary fractions in more distant,

---

<sup>1</sup>For brevity, by ‘binaries’ we generally also mean ‘multiples’, since many stars are found in triple and higher-order multiple systems. We will distinguish the two only when it is important to do so. Note that the analysis in this paper is of *binary* systems.

massive clusters have not yet been studied thoroughly, because these environments are too crowded and their distances too great, so that their member stars are too faint to be examined individually for binarity. Fortunately, there is an alternative approach, i.e., by means of an artificial-star-test technique, which allows us to estimate the binary fractions in crowded environments. By studying the morphology of their color-magnitude diagrams (CMDs), Romani & Weinberg (1991) determined the observed binary fractions in M92 and M30 at  $\lesssim 9$  and  $\lesssim 4\%$ , respectively, for the full populations of cluster stars down to  $m_V \sim 23$  and  $\sim 22$  mag, respectively, based on two-dimensional maximum-likelihood analysis. Rubenstein & Bailyn (1997, hereafter RB97) investigated the binary fraction of main-sequence stars with  $15.8 < V < 28.4$  mag in the  $\sim 13.5$  Gyr-old (e.g., Pasquini et al. 2007) post-core-collapse Galactic globular cluster NGC 6752. They found a binary fraction of 15–38% inside the inner core radius, falling to  $\lesssim 16\%$  at larger radii, with a power-law mass-ratio distribution. For other old globular clusters, Bellazzini et al. (2002) estimated the binary fraction in NGC 288 for stars with  $20 < V < 23$  mag (corresponding to masses of  $0.54 \lesssim M_*/M_\odot \lesssim 0.77$ ) at 8–38% inside the cluster’s half-mass radius (and at  $< 0.10$  in the outer regions, most likely close to zero), regardless of the actual mass-ratio distribution. Zhao & Bailyn (2005) claimed 6–22% of main-sequence binaries ( $19.2 \leq m_{F555W} \leq 21.2$  mag) for M3, within the cluster’s core radius, and between 1 and 3% for stars between 1 and 2 core radii. By applying similar techniques to the post-core-collapse Galactic globular cluster NGC 6397, Cool & Bolton (2002) derived a binary fraction of 3% for main-sequence stars with primary masses between  $0.45$  and  $0.80M_\odot$ , for a range of mass ratios. Based on an extrapolation to all mass ratios, they estimated the total main-sequence binary fraction in the cluster core at 5 to 7%. Davis et al. (2008), using the method pioneered by Romani & Weinberg (1991) in combination with numerical simulations by Hurley et al. (2007), concluded that the outer regions of this cluster (at 1.3–2.8 half-mass radii) exhibit a binary fraction ( $1.2 \pm 0.4\%$ ) close to the primordial fraction of  $\sim 1\%$  predicted by the simulations,

while the inner region has a substantially higher fraction,  $5.1 \pm 1.0\%$ . However, *all clusters thus far studied in this way are old stellar systems* (cf. table 1 in Davis et al. 2008) in which dynamical evolution is expected to have significantly altered the initial binary population.

In this paper, we use accurate photometric observations of the young, low-metallicity star cluster NGC 1818 in the Large Magellanic Cloud, taken with the Wide Field and Planetary Camera-2 (WFPC2) on board the *Hubble Space Telescope (HST)*, to study its binary fraction. The photometric data and the cluster CMD are discussed in §2. Our newly developed method to correct for stellar blends and superpositions, based on the artificial-star-test technique, is presented in §3. The fitting of the binary fraction is discussed in §4, and §5 contains a further discussion and our conclusions.

## 2. Observations, data reduction, and background decontamination

Our data set was obtained from *HST* program GO-7307 (PI Gilmore), which included three images in both the F555W and F814W filters (with exposure times of 800, 800, and 900s per filter). Specifically, we used the observations with the PC1 chip centered on the cluster’s half-light radius (see Fig. 1). The origin of this data set and the program’s scientific rationale were described in detail in de Grijs et al. (2002a, and references therein). The observations were reduced with *HSTPHOT* (version 1.1, May 2003; Dolphin 2002) using the point-spread-function (PSF)-fitting option. Bad and (close to) saturated pixels were masked using data-quality images. Cosmic rays were removed using *HSTPHOT*’s *CRMASK* routine. The three images were combined into a single deep frame (with a total exposure time of 2500s) using the *COADD* routine and hot pixels were removed following the procedure recommended in the *HSTPHOT* manual. Photometry was performed on both the F555W and F814W images simultaneously, using a weighted PSF fit (option ‘2048’ in *HSTPHOT*), as suggested by Holtzman et al. (2006). The instrumental magnitudes

were converted to the standard Johnson/Cousins  $V$  and  $I$  filters using the transformation solutions of Dolphin (2000).

We show the CMD around the cluster’s half-light radius (as defined in HST program GO-7307) in Fig. 2 (left-hand panel) and provide the current-best estimates of a few important cluster parameters including the core and half-mass radii, in Table 1, as well as the relevant bibliographic references. We use the Padova isochrones (Girardi et al. 2000) to perform our fits to the cluster’s CMD (see Fig. 3, left-hand panel). For comparison, we also show the CMD obtained by Liu et al. (2009; see also de Grijs et al. 2002a) using the IRAF APPHOT (aperture photometry) software package in Fig. 2 (right-hand panel). Our newly determined CMD is cleaner and the main sequence is much tighter than that of Liu et al.’s (2009) CMD, because the HSTphot software package we used is much better at properly handling stellar photometry in crowded fields than IRAF’s APPHOT routine, while our PSF-fitting approach ensures higher-precision photometric measurements than Liu et al.’s (2009) aperture photometry (cf. Fig. 2). We will provide a careful, quantitative comparison of the results from both approaches in Hu et al. (in prep.).

As noted by Castro et al. (2001), an old red-giant population and an intermediate-age red-giant clump are clearly seen in the CMD of NGC 1818. If we adopt an age for this cluster of approximately 25 Myr (e.g., de Grijs et al. 2002a; and references therein), these older components can only be interpreted as background field stars in the LMC’s disk. Therefore, the main sequence of NGC 1818 is severely contaminated by field stars. Here, we adopt a statistical approach similar to that adopted by Bonatto et al. (2006) to subtract background stars. The background data set (to which we applied exactly the same photometric procedures as for our science field) was obtained as part of *HST* program GO-6277 (PI Westphal); it is suitably located at a distance of  $\sim 8$  arcmin from the cluster’s

half-mass radius.<sup>2</sup> The middle panel of Fig. 3 shows the CMD of the LMC background field near NGC 1818, which was specifically observed for background characterization (see, for more details, Castro et al. 2001; Santiago et al. 2001; de Grijs et al. 2002a). We only remove the stars in the region  $19 \leq V \leq 25$  mag and  $-0.1 \leq (V - I) \leq 1.5$  mag, since this region contains almost all stars for which the observational completeness fraction is greater than 50%. To perform the field-star decontamination procedure, we divide both the background and cluster CMDs into grids of cells, in color and magnitude. We count the number of stars in each cell in the background CMD, and then randomly remove the corresponding number of stars, corrected for the difference in area covered, from the respective cell of the cluster CMD. The choice of cell size affects the appearance of the resulting background-subtracted cluster CMD significantly. After extensive experimentation we chose a cell size of three times the observational uncertainty in both magnitude and color of single stars (i.e.,  $3\sigma = 0.06$  mag) to minimize any significant effects due to stochasticity. The right-hand panel of Fig. 3 shows the results of the background decontamination.

We performed additional tests to validate our approach, based on the simplest assumption that if we subtract the background stellar population from the original background field, we should be left with only statistical noise, which should, therefore, not lead to systematics in our analysis. These tests indeed showed that our background-subtraction procedure is robust. Nevertheless, a close examination of the right-hand panel of Fig. 3 shows that there is some residual contamination from the background stellar population, as indicated by the presence of a faint red-giant branch/clump feature. This is

---

<sup>2</sup>We initially selected a number of suitable LMC fields for our background subtraction, including the field specifically associated with the cluster from *HST* program GO-7307. Eventually, we decided to use the field that best represented the background isochrone shown in the left-hand panel of Fig. 2.

most likely caused by the local background in the cluster region being somewhat different from that in our comparison field (we applied two slightly different field regions in an attempt to optimally subtract the local cluster background, but a small residual effect remains). For the statistical comparison carried out in the remainder of this paper, we are confident that this residual background population affects our results negligibly, however. We base this conclusion on (i) the fact that the dominance of the background population is significantly redward with respect to the expected locus of NGC 1818’s main-sequence binary population (i.e., the residual background contamination dominates the region *outside* the parallelogram shown in the right-hand panel of Fig. 3; our background-subtraction procedure at and near the single- and binary-star main sequence is unaffected by these stellar types) and (ii) a statistical analysis of the relative importance of the genuine binaries versus the residual background contamination: we estimate that in the region in the CMD space of interest (i.e., the parallelogram), the fractional contamination by the background population (i.e., our systematic error) is  $\lesssim 3\%$  (based on a detailed examination of the stellar population using star counts). Finally, in Fig. 4 we present the completeness curves for both the NGC 1818 observations and the background field, for two of the four WFPC2 chips. We emphasize that we performed completeness analyses for all four chips, so that we can properly and consistently correct our observational data for the effects of incompleteness. We also note that for the entire magnitude range of interest,  $V \lesssim 22$  mag (see the parallelogram in Fig. 3), the completeness of our data is well in excess of 80%, so that corrections for incompleteness are straightforward.

### 3. Artificial-star tests

Ideally, if there is no binary population, nor any observational errors, all stars in a cluster should lie on the same isochrone, because they were all born at approximately the

same time in the same giant molecular cloud (i.e., they have the same metallicity). However, in Fig. 3 we clearly see a broadening of the cluster’s main sequence. There are three factors that contribute to this broadening: (i) photometric errors, (ii) superposition effects, and (iii) the presence of true binary and/or multiple systems. Photometric errors broaden the main sequence symmetrically if we assume the magnitude errors to be Gaussian, which is not unreasonable (given that the magnitude range of interest is well away from the observational completeness limit). However, the other two factors skew the stars to the brighter, and redder, side relative to the corresponding best-fitting isochrone. However, it is difficult to distinguish between superpositions and physical binaries on the basis of only CMD morphological analysis. To obtain the binary fraction of NGC 1818, we therefore perform Monte Carlo tests, where we produce artificial-star catalogs and compare the spread of real and artificial stars around the best-fitting isochrone.

Since the photometric errors of the observed stars strongly depend on their magnitudes and their positions on the *HST*/WFPC2 chips used for the observations, exponential functions (numerically following the densest concentration of data points, closely matched to their lower boundary) were adopted to fit the relation between the magnitude and standard deviation of the photometric errors (these relations vary between the WFPC2 chips; we have taken great care to use the appropriate relations for our analysis). Each artificial star (see below) is randomly assigned Gaussian photometric errors, of which the standard Fig. 5 shows the photometric uncertainties as a function of  $V$  and  $I$  magnitude for the *HST*/WF3 observations (containing 2473 stars); the center of the corresponding PC1 chip (containing 886 stars) is located at the half-light radius. The solid curves in Fig. 5 show the functions adopted to assign uncertainties to the individual artificial stellar magnitudes; 80% of the data points are located within  $\sim 1.2$  times the standard deviation from the curve.

The global stellar mass function of NGC 1818 is well approximated by a Salpeter (1955) power law for masses  $> 0.6M_{\odot}$  (de Grijs et al. 2002b; Kerber et al. 2007; Liu et al. 2009).<sup>3</sup> Therefore, we draw the masses of single stars and the primary stars of the binary population from a Salpeter (1955)  $\alpha = 2.35$  power-law IMF in the mass range  $0.6 \leq M_{\star}/M_{\odot} \leq 6.0$ . The masses of the secondaries are drawn from a given mass-ratio distribution for all primary masses (we discuss the choice of the mass-ratio distribution in detail in the next section). We note that this produces a *total* IMF (of single stars plus each component of binary systems) which is *not* equal to a Salpeter IMF. However, the deviation from a Salpeter IMF is fairly minor (see Kerber et al. 2007). The alternative is to draw both primary and secondary masses from a Salpeter IMF. However, random pairing is excluded in all observed multiple populations (see, e.g., Duquennoy & Mayor 1991; Fischer & Marcey 1992; Kouwenhoven et al. 2005; Duchêne et al. 2007).

The magnitudes and colors of all artificial stars are then obtained by interpolating from the relevant isochrone. For binary stars, we simply add the fluxes of the primaries and secondaries to obtain the magnitudes and colors of the system. The results from this procedure are shown in Fig. 6 (left-hand panel).

The best way to simulate the superposition effect is by adding artificial stars to the

---

<sup>3</sup>We note that these mass-function fits were obtained on the basis of a single-star mass-function assumption. However, as Kerber et al. (2007; see also Liu et al. 2009) illustrate in their Fig. 9, the inclusion of binaries affects the derived mass-function slope only slightly: the deviation between the input (single-star) and output (single+binary) mass functions they derive is less than 0.15 (in units of the mass-function slope,  $\alpha$ ), as long as the input slope is sufficiently close to the Salpeter (1955) index and assuming a 100% binary fraction. A smaller binary fraction, as found in this study, will change the mass-function slope proportionately less (see Kerber et al. 2007).

original images (see details in RB97; and references therein). Alternatively, in each run we randomly distribute  $5 \times 10^6$  artificial stars on the spatial-distribution diagram of the real stars (while properly accounting for the position-dependent photometric uncertainties using the chip-dependent magnitude–uncertainty relations discussed above), instead of on the original images. If an artificial star has an angular distance from any real star within 2 pixels (corresponding to the size of our aperture), it is assumed to be ‘blended’ [see below; see also Reipurth et al. (2007) for a blending analysis relevant to this study]. Its new magnitude and color are re-calculated in the same way as for a binary system. To avoid double counting, if the output  $V$ -band magnitude of any artificial star is 0.752 mag brighter than its input magnitude (as expected for equal-mass binary systems), we assume that we are dealing with a chance superposition and remove the star from the output catalog. However, we do not allow the artificial stars to blend with each other, even when their angular distance is less than 2 pixels. Therefore, we do not need to add artificial stars multiple times to avoid blends between them. This is one of the main differences between our novel approach and that followed by RB97 (the latter authors added much smaller numbers of artificial stars to their images, precisely to avoid this blending issue).<sup>4</sup> The CMDs of the artificial stars are shown in Fig. 6. Fig. 8 presents a comparison of the observed, background-subtracted CMD with the artificial CMD containing 50% binaries. By adding artificial stars to the raw images, we robustly verified that the 2-pixel threshold we adopted is a good approximation to simulate stellar blending (see Hu et al., in prep., for the full quantitative analysis).

---

<sup>4</sup>Using this approach, we can generate any number of artificial stars, with which we can construct an artificial-star catalog that has the same luminosity function and spatial distribution as the observations, thus requiring much less computing time than when using the full images for our analysis.

For each observed star, we find all artificial stars in the input catalog that are located within 20 pixels and within 0.2 mag in brightness.<sup>5</sup> We randomly extract one of these artificial stars as the counterpart to the observed star. Finally, we construct a synthetic catalog containing the same total number of *systems* (be they single stars or unresolved binary systems), a similar luminosity function, projected surface number density, and superposition probability as the original data. The only differences between the observed and synthetic catalogs are the binary properties (both the binary fraction and the mass-ratio distribution).

#### 4. The binary fraction of NGC 1818

We analyze stars in the mass range from  $1.3$  to  $1.6M_{\odot}$  (roughly F stars), in the region of the CMD in the parallelogram shown in the right-hand panel of Fig. 3, which is where any binary sequence will show optimally. For brighter stars, the isochrone is almost vertical, and therefore the binary sequence is too close to the main sequence to allow us to distinguish it. (In addition, we are not fully convinced that all these bright stars are really main-sequence stars rather than blue stragglers.) For fainter stars, the larger photometric errors and lower completeness make it difficult to detect the binary population. (As we noted above, we applied position-dependent completeness corrections to our data, which

---

<sup>5</sup>This choice is driven by the need to have a statistically sound procedure: we generated artificial stars that may or may not fall exactly on top of a real star. Therefore, we needed to choose a region around any real star in which any artificial star(s) correspond(s) to the real star for statistical comparison purposes. RB97 used stars within 100 pixels, but since we are less restricted by computational power, a smaller radial range ensures that the spatial distributions of the real stars and the final catalog of artificial stars are statistically the same.

were all  $> 80\%$  complete in the magnitude range of interest.) Since the isochrone is almost linear in the region in CMD space of interest, we rotate the ordinates of the artificial and observed CMDs such that the isochrone becomes vertical to a new ‘pseudo-color,’ i.e., a new function of  $V$  and  $V - I$  produced by rotating the CMD (corresponding to the color axis projected onto the long side of the parallelogram in Fig. 2). Note that the exact form of the pseudo-color function is unimportant.

In Fig. 9 we show the cumulative distribution function (CDF) with pseudo-color of the true CMD (solid line) and a stellar population with photometric errors, but *no* binaries (dotted line).<sup>6</sup> This is clearly a very poor fit to the data. We also show the best-fitting binary fraction ( $f_b$ ), with a uniform  $q$  distribution, of  $f_b = 0.55 \pm 0.05$  ( $1\sigma$ ) (dashed line), as well as the relevant model for 100% binarity (long-dashed line).

It is expected that this method will be insensitive to low- $q$  systems in which the secondary component contributes very little to the pseudo-color. To test our sensitivity to the mass ratio of a system, we produce artificial catalogs that do not include binaries below some mass ratio  $q_{\text{cut-off}}$ , but contain the same number of binaries above  $q_{\text{cut-off}}$ . Therefore, we need to compare these results based on the artificial-star catalogs with the best-fitting  $f_b = 0.55$  with  $q_{\text{cut-off}} = 0$  (see Fig. 9).

We find that there is very little difference in the fits to the CDF for  $q_{\text{cut-off}} < 0.4$ , showing that we are insensitive to binaries with mass ratios smaller than  $q \sim 0.4$ . In Fig. 9 we plot the binary fraction versus  $\chi^2$  probability (rms error) for different  $q_{\text{cut-off}}$ ’s. For  $q_{\text{cut-off}} < 0.4$ , the best fits of binary fraction are acceptable, since the maximum

---

<sup>6</sup>As the luminosity function of the final output artificial stars is similar to the observed luminosity function, the precise form of the stellar mass function is unimportant in this context.

probabilities are much larger than the commonly adopted limit of  $\Delta\chi^2 = 0.05$ .<sup>7</sup> However, for  $q_{\text{cut-off}} = 0.5$ , the value is just a little greater than 0.02. And for  $q_{\text{cut-off}} = 0.7$ , the very low  $\chi^2$  value indicates that even the best fit is poor. Therefore, we adopt a conservative limit to the mass ratios to which we are sensitive of  $q > 0.4$ .

For this discussion, we have assumed that the  $q$  distribution is flat (at least above  $q = 0.4$ ). This is consistent with the mass-ratio distribution of A- and B-type stars in Sco OB2 (Kouwenhoven et al. 2005, their fig. 14). However, G-dwarf mass ratios in the solar neighborhood are concentrated toward low  $q$  (Duquennoy & Mayor 1991). Duquennoy & Mayor (1991) show that the mean local G-dwarf  $q$  distribution shows a roughly linear decrease with increasing  $q$  for  $q > 0.4$  (their fig. 10).

The results indicate that the *total* binary fraction of F stars in NGC 1818 is  $\sim 0.55$ , with an approximately flat mass-ratio distribution. However, since we are only sensitive to binaries with  $q > 0.4$ , we may only constrain the binary fraction in this mass range to  $f_{b(q>0.4)} \sim 0.35$ . It is impossible to determine the total binary fraction without making some assumptions about the form of the  $q$  distribution below 0.4. It is unlikely that the mass-ratio distribution declines below 0.4, meaning that a total binary fraction of  $\sim 0.55$  is probably a safe lower limit (cf. the mass-ratio distributions found by Duquennoy & Mayor 1991; Kouwenhoven et al. 2007). *Depending on exactly which assumptions are made for the form of the mass-ratio distribution, the total binary fraction ranges from 0.55 to (more probably) unity.*

---

<sup>7</sup>G. E. Dallal (2007), <http://www.jerrydallal.com/LHSP/p05.htm>.

## 5. Discussion and conclusions

The CMD of NGC 1818, obtained from *HST* photometry, shows a clearly asymmetric broadening of the main sequence, which implies that this cluster contains a large fraction of binary systems. Using the artificial-star-test method, we estimate that the binary fraction in the mass range from 1.3 to  $1.6M_{\odot}$  is  $f_b \sim 0.35$  for systems with an approximately flat mass-ratio distribution for  $q > 0.4$ . This is consistent with a *total* binary fraction of F stars of 0.55 to unity. Elson et al. (1998) found the fraction of roughly equal-mass ( $q \sim 1$ ) systems in NGC 1818 to be 30–40% in the core and 15–25% outside the core, which is consistent with our result.

Observationally determined binary fractions are rather scant in general. Binary fractions are a clear function of stellar type, age, and environment. We note that our result is quite close to the fraction of binary dwarfs in the field of the same spectral type, which is a little smaller than the fraction in Sco OB2 (Kouwenhoven 2006) and much higher than in Galactic globular clusters (e.g., RB97; Bellazzini et al. 2002). The most recently published relevant results include the determination by Sana et al. (2008) of the binary fraction of O-type stars in NGC 6231 (at least 63%), while Reipurth et al. (2007) reported a visual-binary fraction of late-type stars in the Orion Nebula Cluster of only 8.8%.

At 15–25 Myr old, NGC 1818 is several crossing times old, and the binary population would be expected to have been modified by dynamical interactions (see Goodwin et al. 2007; and references therein). In particular, soft (i.e., wide) binaries would be expected to have been destroyed by this age. Therefore, the high binary fraction found for F stars suggests that these binaries are relatively ‘hard’ and able to survive dynamical encounters.<sup>8</sup>

---

<sup>8</sup>We argue that the binaries in NGC 1818 must be ‘hard,’ since the cluster is dynamically old and soft binaries are destroyed in roughly a crossing time (e.g., Parker et al. 2009), so

The relatively flat mass-ratio distribution in NGC 1818 compared to similar-mass stars in the loose association Sco OB2 (Kouwenhoven et al. 2007;  $\sim q^{-0.4}$ ) may be evidence for a difference in the initial populations (see also Sana et al. 2008 for an alternative mass-ratio distribution biased toward unity). However, it is more likely to be a product of the different dynamical evolution of the two populations. The larger number of encounters suffered by the binary population in NGC 1818 would be expected to disrupt less-bound (i.e., wide and/or low- $q$ ) systems, and to form more equal-mass systems, leading to a mass-ratio distribution more biased to high  $q$ .

We conclude that the binary fraction of F stars in the young, low-metallicity LMC cluster NGC 1818 is high and consistent with the field and lower-density clusters. This suggests that, at least among intermediate-mass stars, metallicity down to  $[\text{Fe}/\text{H}] \sim -0.4$  dex does not suppress fragmentation and binary formation, and the binarity of these stars is at least as high as at solar metallicity.

We gratefully acknowledge joint networking funding from the Royal Society in the UK and the National Natural Science Foundation of China (NSFC), supporting a UK-China International Joint Project between the University of Sheffield and the National Astronomical Observatories (Chinese Academy of Sciences) of China. YH, LD, and QL acknowledge financial support from NSFC grants 10973015 and 10778719, and the Ministry of Science and Technology of China grant 2007CB815406. RdG acknowledges NSFC grant 11043006. He also acknowledges financial assistance from the Kavli Institute for Astronomy and Astrophysics prior to moving from the UK to China. This research has made use of NASA’s Astrophysics Data System Abstract Service. We also thank Thijs Kouwenhoven

---

soft binaries cannot be a major component of the binary population (some may form by capture but will be quickly destroyed).

for useful discussions and valuable input. Finally, RdG and LD pay tribute to the 2003 Guillermo Haro workshop for initiating their collaboration, having thus far resulted in 2 PhD theses and numerous secondary benefits. This turned out to be a career-defining moment for RdG.

## REFERENCES

- Abt H. A., 1983, *ARA&A*, 21, 343
- Bate M. R., 2005, *MNRAS*, 363, 363
- Bellazzini M., Fusi Pecci F., Messineo M., Monaco L., Rood R. T., 2002, *AJ*, 123, 1509  
1994, *Galactic Dynamics*, Princeton: Princeton University Press
- Bonatto C., Santos J. F. C., Bica E., 2006, *A&A*, 160, 83
- Castro R., Santiago B. X., Gilmore G. F., Beaulieu S., Johnson R. A., 2001, *MNRAS*, 326,  
333
- Cool A. M., Bolton A. S., 2002, in: *A.S.P. Conf. Ser. Vol. 263, Stellar Collisions, Mergers  
and Their Consequences*, ed. M. M. Shara (San Francisco: ASP), p. 163
- Correia S., Zinnecker H., Ratzka Th., Sterzik M. F., 2006, *A&A*, 459, 909
- de Grijs R., Johnson R. A., Gilmore G. F., Frayn C. M., 2002a, *MNRAS*, 331, 228
- de Grijs R., Gilmore G. F., Johnson R. A., Mackey A. D., 2002b, *MNRAS*, 331, 245
- Dolphin Andrew E., 2000, *PASP*, 112, 1383
- de Grijs R., 1999, *A&A*, 341, 547
- de Grijs R., Delgado-Donate E., Haisch K. E. Jr., Loinard L., Rodríguez L. F., 2007, in:  
*Protostars and Planets V*, B. Reipurth, D. Jewitt, and K. Keil, eds., (Univ. of  
Arizona Press: Tucson), p. 379
- Duquennoy A., Mayor M., 1991, *A&A*, 248, 485
- Elson R. A. W., Hut P., Inagaki S., 1987, *ARA&A*, 25, 565

- Elson R. A. W., Sigurdsson S., Davies M., Hurley J., Gilmore G., 1998, MNRAS, 300, 857
- Fischer D. A., Marcy G. W., 1992, ApJ, 396, 178
- Girardi L., Bressan A., Bertelli G., Chiosi C., 2000, A&AS, 141, 371
- Goodwin S. P., Kroupa P., 2005, A&A, 439, 565
- Goodwin S. P., Kroupa, P., Goodman, A. & Burkert, A. 2007, in: Protostars and Planets V, B. Reipurth, D. Jewitt, and K. Keil, eds., (Univ. of Arizona Press: Tuscon), p. 133
- Goodwin S. P., Nutter D., Kroupa, P., Ward-Thompson D., Whitworth A. P., 2007b, A&A, 477, 823
- Hut P., et al., 1992, PASP, 104, 981
- Holtzman Jon A., Afonso C., & Dolphin A., 2006, ApJS, 166, 534
- Hunter D. A., Light R. M., Holtzman J. A., Lynds R., O’Neil E. J. Jr., Grillmair C. J., 1997, ApJ, 478, 124
- Johnson R. A., Beaulieu S. F., Gilmore G. F., Hurley J., Santiago B. X., Tanvir N. R., Elson R. A. W., 2001, MNRAS, 324, 367
- Kerber L. O., Santiago B. X., Brocato E., 2007, A&A, 462, 139
- Korn A. J., Becker S. R., Gummersbach C. A., Wolf B., 2000, A&A, 353, 655
- Kouwenhoven M. B. N., Brown A. G. A., Zinnecker H., Kaper L., Portegies Zwart S. F., 2005, A&A, 430, 137
- Kouwenhoven M. B. N., 2006, Ph.D. Thesis, University of Amsterdam (astro-ph/0610792)

- Kouwenhoven M. B. N., Brown A. G. A., Portegies Zwart S. F., Kaper L., 2007, *A&A*, 474, 77
- Kouwenhoven M. B. N., Brown A. G. A., Zinnecker H., Kaper L., Portegies Zwart S. F., 2005, *A&A*, 430, 137
- Kroupa P., Petr M. G., McCaughrean M. J., 1999, *NewA*, 4, 495
- Lada C. J., Lada E. A., 2003, *ARA&A*, 41, 57
- Parker R. J., Goodwin S. P., Kroupa P., Kouwenhoven M. B. N., 2009, *MNRAS*, 397, 1577
- Pasquini L., Bonifacio P., Randich S., Galli D., Gratton R. G., Wolff B., 2007, *A&A*, 464, 601
- Rubenstein E. P., Bailyn C. D., 1997, *ApJ*, 474, 701 (RB97)
- es M. M., Connelley M. S., Bally J., 2007, *AJ*, 134, 2272
- Salpeter E. E., 1955, *ApJ*, 121, 161
- Y., Rauw G., Linder N., 2008, *MNRAS*, 386, 447
- Santiago B., Beaulieu S., Johnson R., Gilmore G. F., 2001, *A&A*, 369, 74
- Tokovinin, A. A., Smekhov M. G., 2002, *A&A*, 382, 118
- Zhao B., Bailyn C. D. 2005, *AJ*, 129, 1934

Table 1: Fundamental parameters of NGC 1818

Parameter	Value	Ref.
$\log(\text{age}/\text{yr})$	$7.2 \pm 0.1$	2
	$7.4 - 7.6$	5
$[\text{Fe}/\text{H}]$ (dex)	$-0.4$	6
$E(B - V)$ (mag)	$0.05$	4
$(m - M)_0$ (mag)	$18.58$	1
$\log(t_{\text{rh}}/\text{yr})$	$9.0 - 9.7$	7
Mass ( $M_{\odot}$ )	$3 \times 10^4$	3
$R_{\text{core}}$ (pc)	$2.56$	2
$R_{\text{hl}}$ (pc)	$2.6$	2

REFERENCES: 1, Castro et al. (2001); 2, de Grijs et al. (2002a); 3, Elson et al. (1987); 4, Hunter et al. (1997); 5, Johnson et al. (2001); 6, Korn et al. (2000); 7, Santiago et al. (2001).

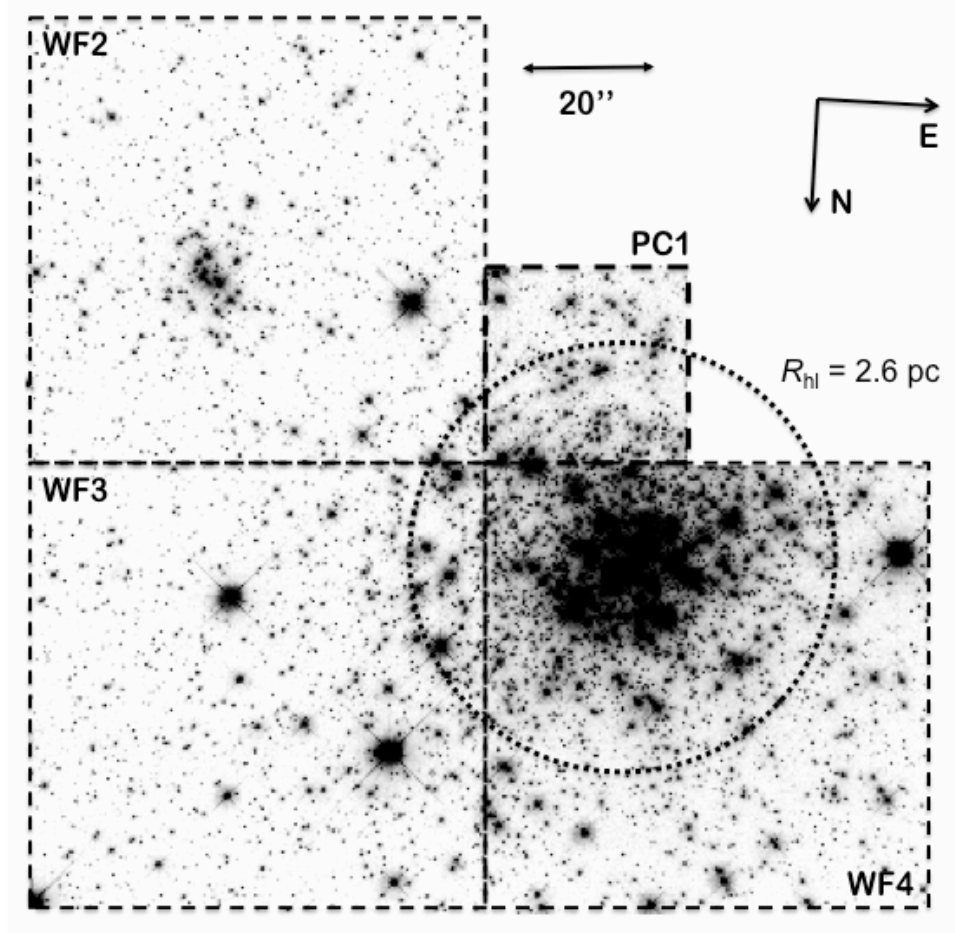


Fig. 1.— Overview of the NGC 1818 field used in this paper. The individual *HST*/WFPC2 chips are labeled, as is the cluster’s half-light radius (dotted circle).

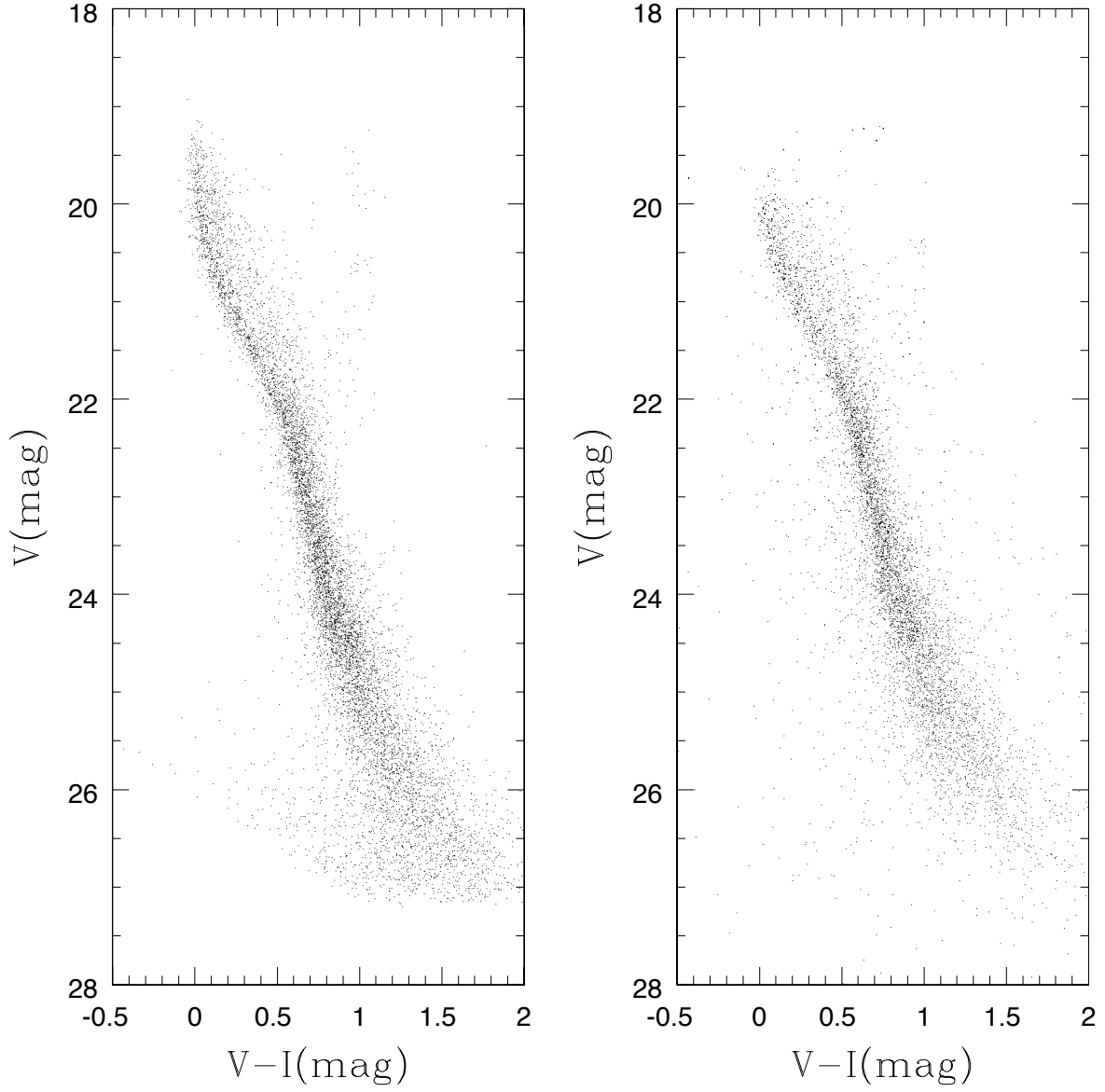


Fig. 2.— *(left)* Our newly determined CMD of NGC 1818 at its half-mass radius. *(right)* CMD from Liu et al. (2009).

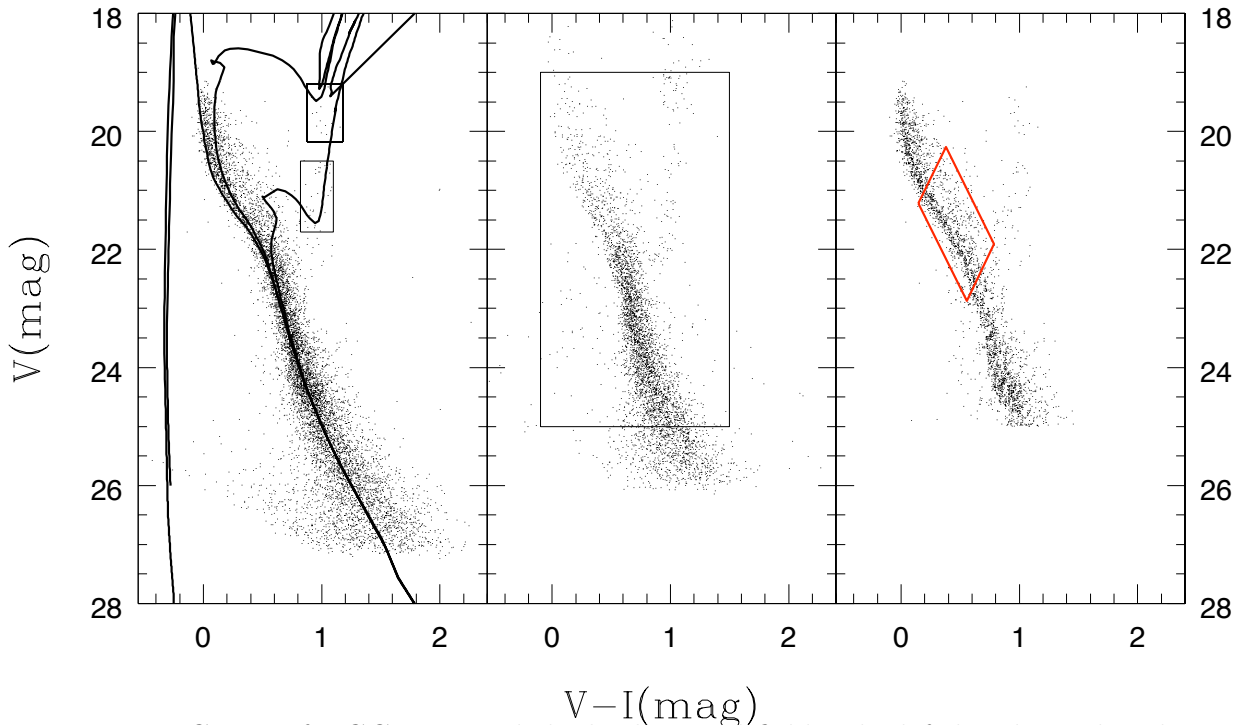


Fig. 3.— CMDs of NGC 1818 and the background field. The left-hand panel is the original CMD. A 25 Myr-old isochrone is used to fit the cluster, and two much older, 0.6 Gyr and 2.5 Gyr isochrones to fit the background red-clump and red-giant stars. All isochrones shown are for a metallicity of  $Z = 0.008$  (cf.  $Z_{\odot} = 0.019$ ). The contribution of the background (field) stars at these evolutionary stages is estimated from star counts in the two rectangular boxes shown in this panel (the upper and lower boxes are used for the red-clump and red-giant stars, respectively). The middle panel shows the CMD of the background field (from which we only use the stars inside the box shown in this panel for the field-star correction done in this paper), and the right-hand panel is the decontaminated CMD of NGC 1818. Our analysis of the binary fraction of NGC 1818 is confined to the stars in the parallelogram indicated in the right-hand panel, which covers stars with masses from 1.3 to 1.6  $M_{\odot}$ . We note that in the region of CMD space of interest (the parallelogram in the right-hand panel), the completeness fraction of our data is well in excess of 80% for the faintest stars, irrespective of position in the cluster.

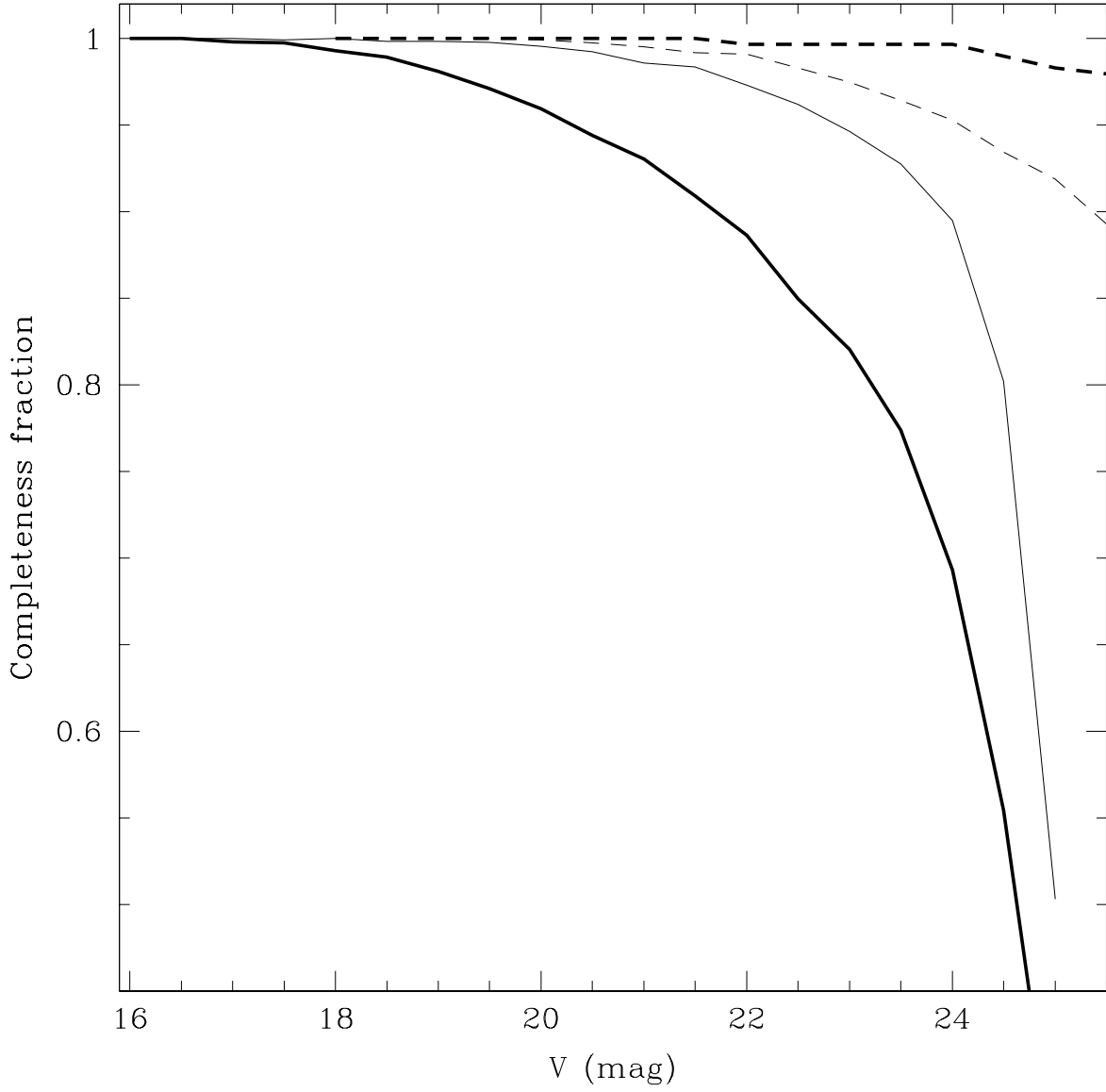


Fig. 4.— Completeness curves for our NGC 1818 observations (solid lines) and the background field (dashed lines). The thick curves are for the PC chip and the thin curves represent the data for the WF3 chip.

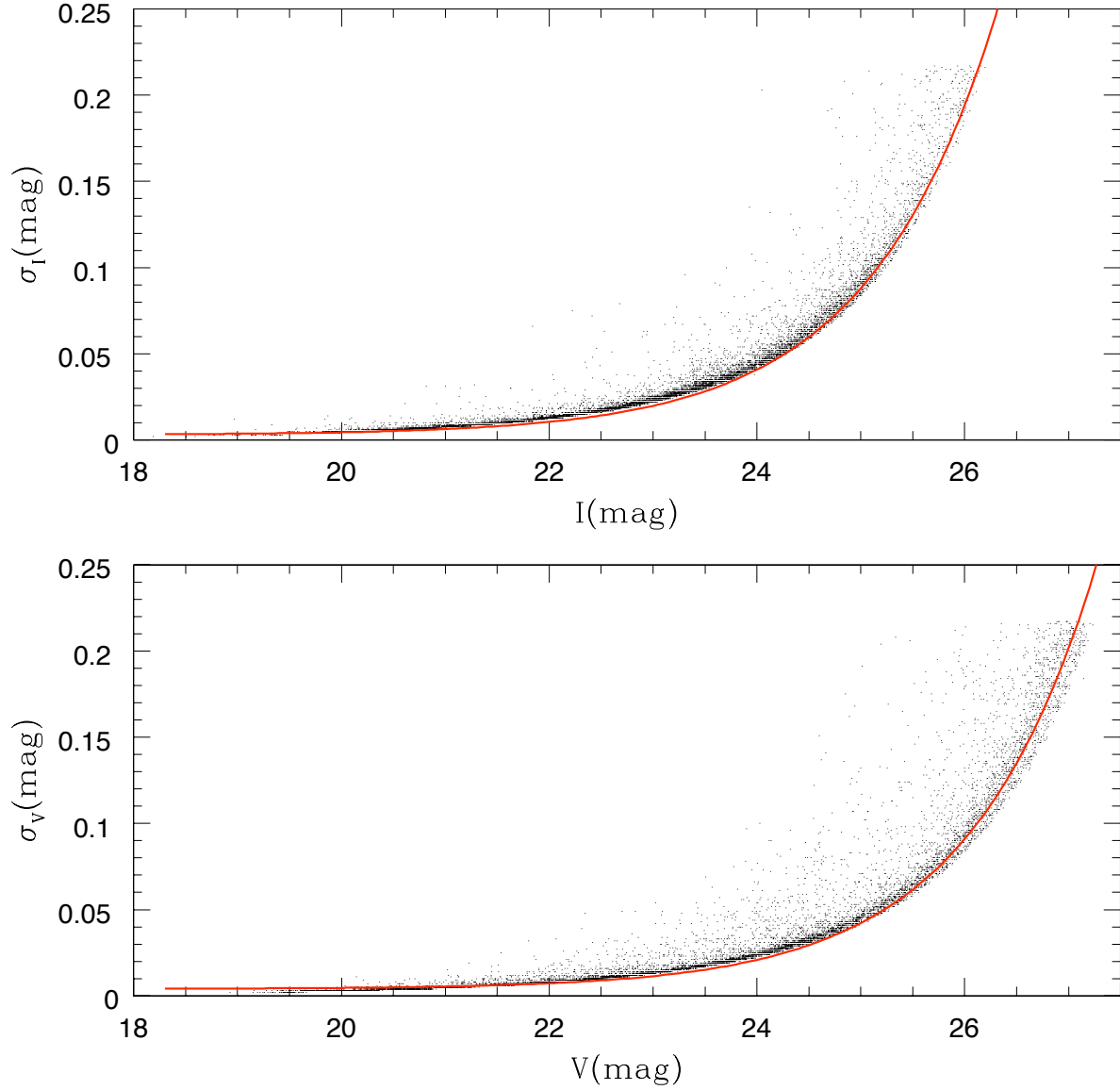


Fig. 5.— Relations between the standard deviations of the photometric uncertainties and stellar magnitudes for the WF3 chip. The solid lines are the best exponential fits to the lower boundaries of the data points for  $V, I < 25$  mag.

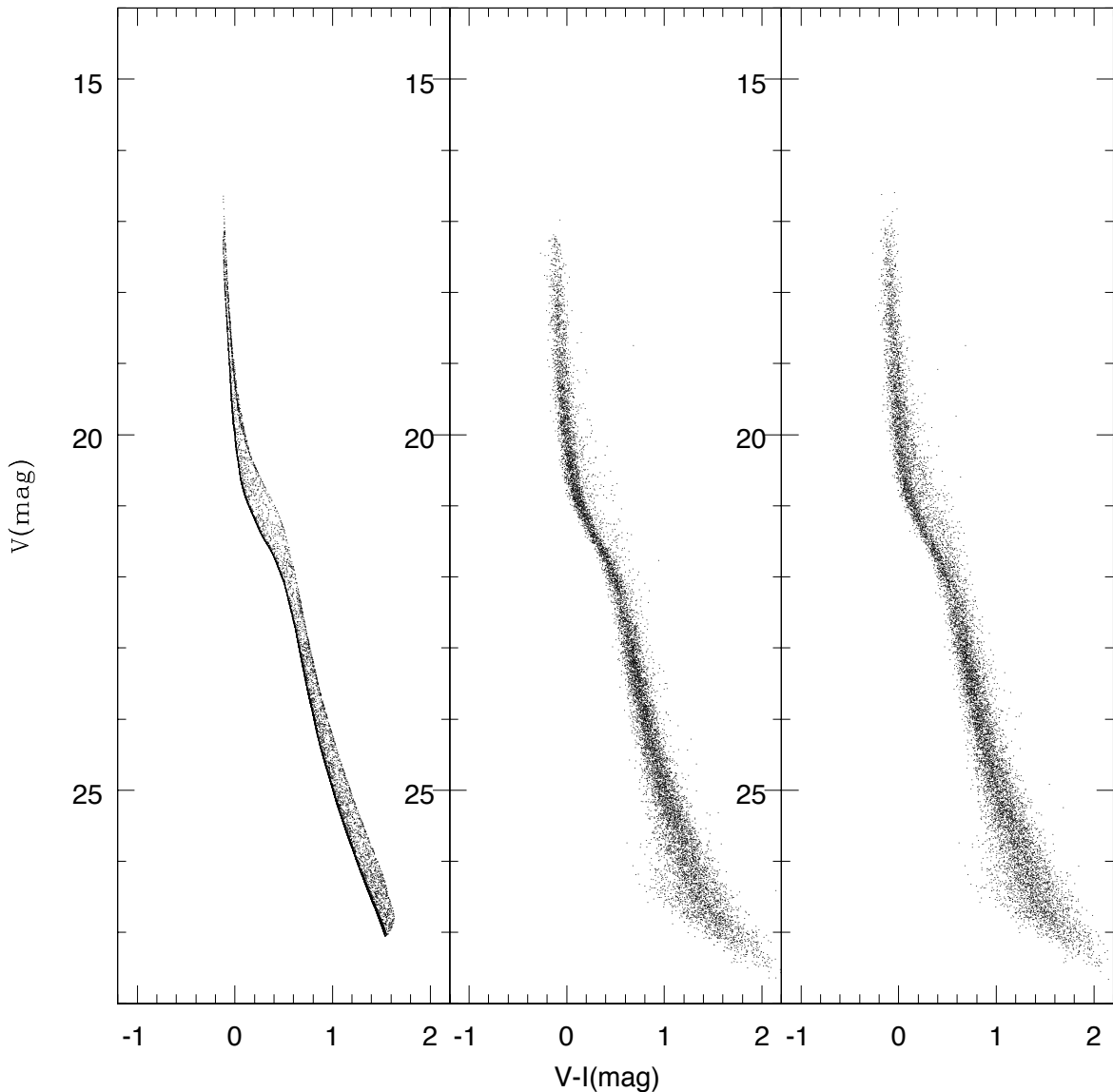


Fig. 6.— *(left)* CMD of the artificial stars without the inclusion of errors, and a 50% binary fraction. An equal-mass binary sequence 0.752 mag brighter than the main sequence can be seen clearly. *(middle)* CMD of the artificial stars with Gaussian photometric errors, but without any binaries. *(right)* CMD of the artificial stars with a 50% binary fraction *and* Gaussian photometric errors. (Note that without any binaries, a ‘binary sequence’ is also observed in the CMD. The number of real stars above the binary sequence plus the  $1\sigma$  observational uncertainty is 12%. For artificial star clusters with a 55% binary fraction this number is approximately 7%, while there are nearly no stars at these loci for artificial clusters with a 0% binary fraction)

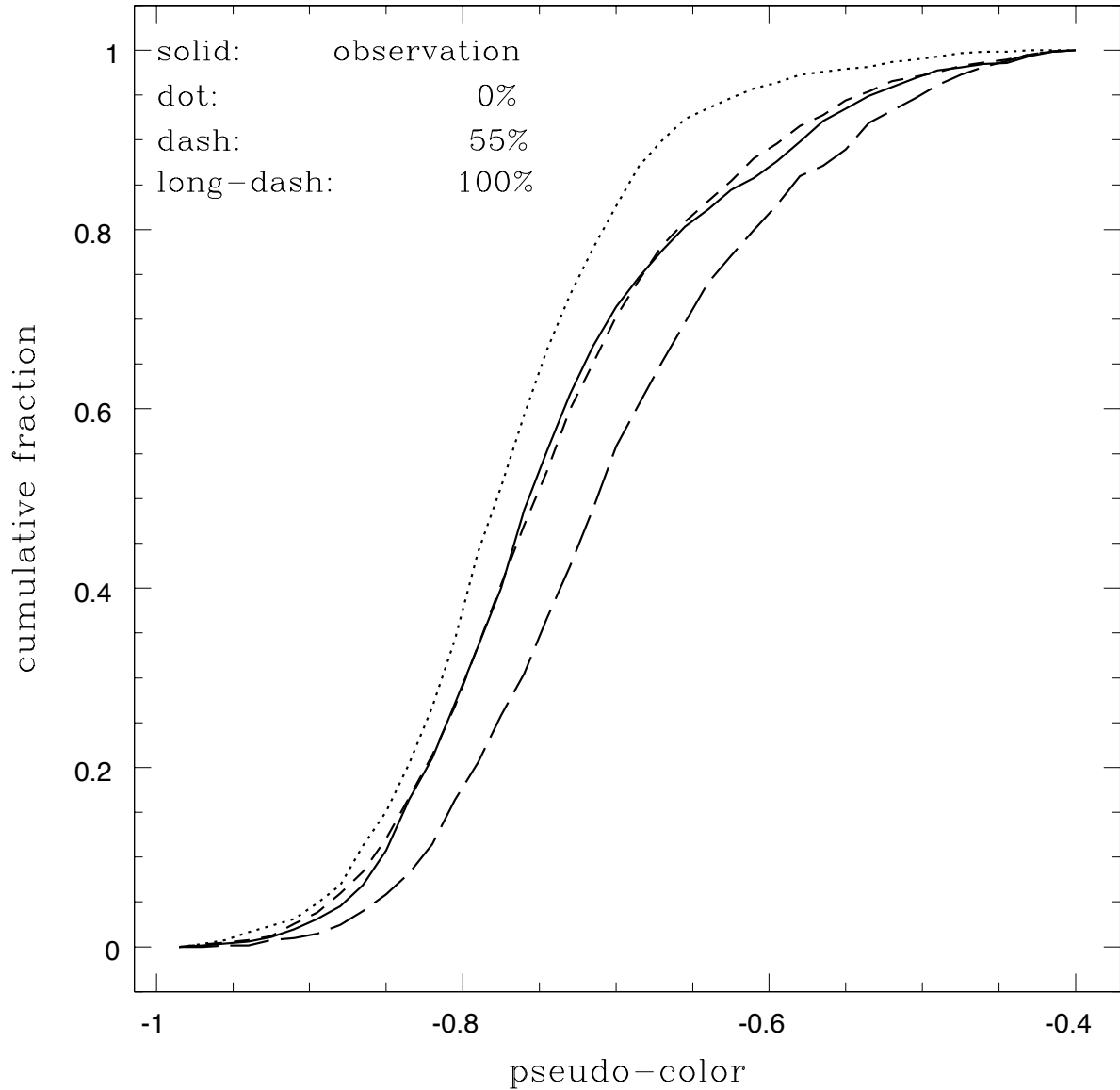


Fig. 7.— Comparison of the observed and best-matching artificial-star CMDs. (*top left*) Background-subtracted observed CMD (equivalent to the right-hand panel of Fig. 3). (*top right*) Artificial CMD with a 50% binary fraction (see the right-hand panel of Fig. 6). The bottom panels show the pseudo-color–pseudo-magnitude diagrams (see §4 for details) of both the real and artificial stars within the parallelogram region indicated in Fig. 3.

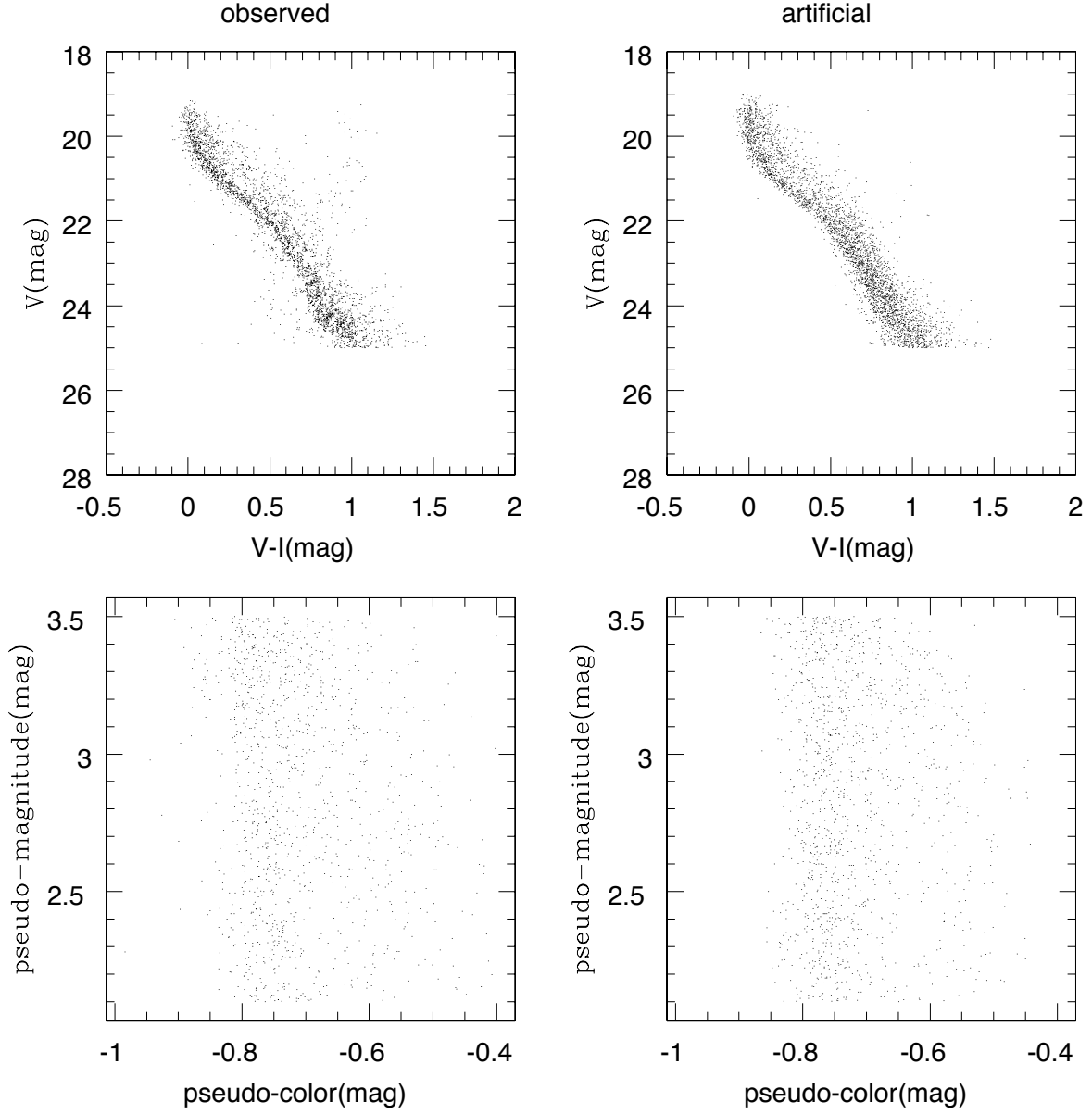


Fig. 8.— Observed cumulative distribution function with pseudo-color (solid line) compared with an artificial stellar population with zero and 100% binary fractions (dotted and long-dashed lines, respectively), and the best-fitting uniform mass-ratio distribution of  $f_b = 0.55 \pm 0.05$  (dashed line).

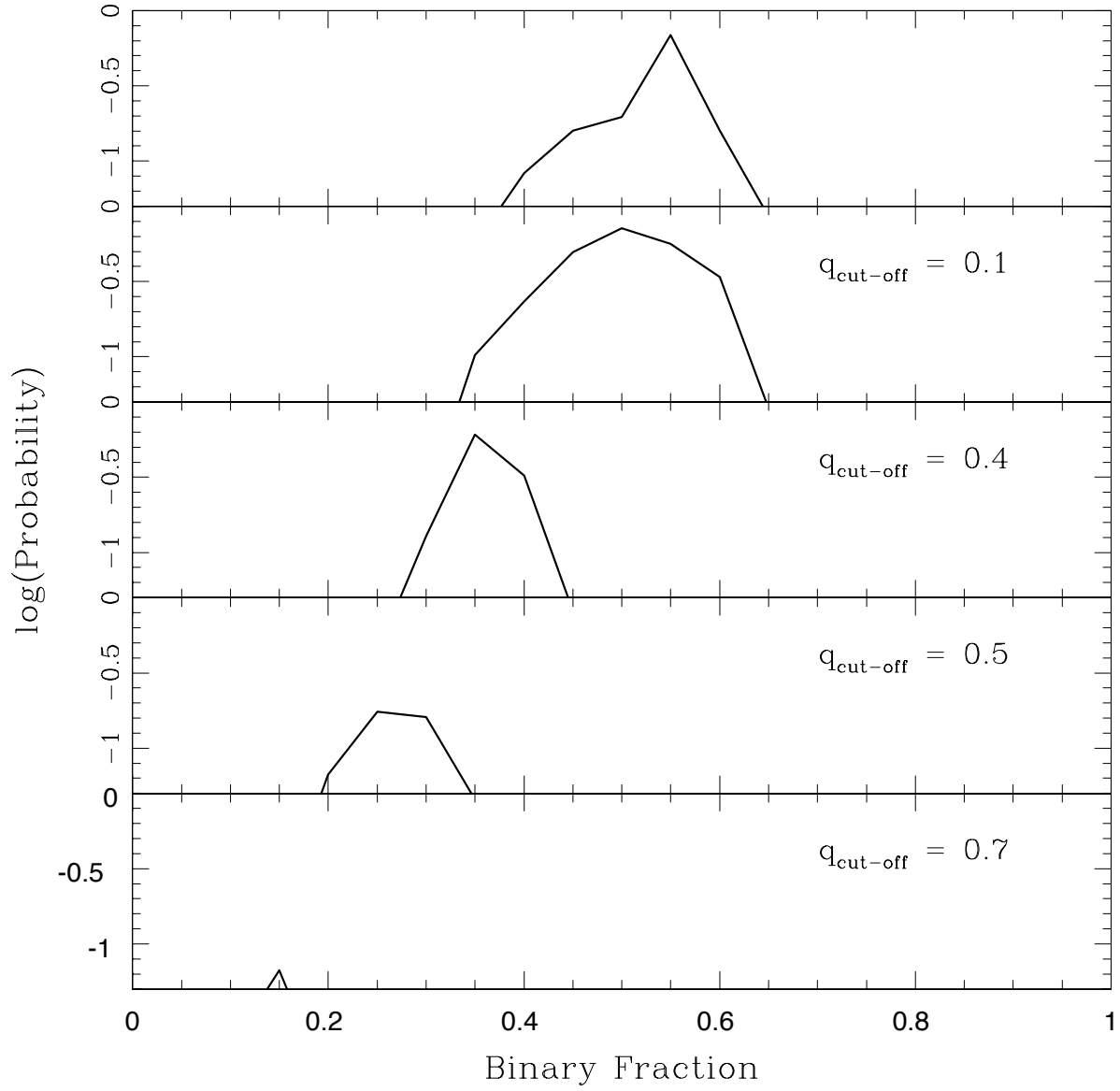


Fig. 9.— Binary fraction and  $\chi^2$  probability for different  $q_{\text{cut-off}}$ . Only probabilities greater than 0.05 are shown.